



Zinc(II)–phenoxyl radical complexes: Dependence on complexation properties of Zn–phenolate species

Yuichi Shimazaki^{a,*}, Tatsuo Yajima^{b,*}, Tadashi Shiraiwa^b, Osamu Yamauchi^b

^a College of Science, Ibaraki University, Bunkyo, Mito 310-8512, Japan

^b Faculty of Chemistry, Materials and Bioengineering, Kansai University, Suita, Osaka 564-8680, Japan

ARTICLE INFO

Article history:

Received 20 August 2008

Received in revised form 29 October 2008

Accepted 4 November 2008

Available online 18 November 2008

Keywords:

Zinc(II) complexes

Phenolate

Complexation

Phenoxyl radical

Stability constants

Nitrogen donors

ABSTRACT

Zinc(II) complexes of N₃O-donor tripodal ligands, 2,4-di(*tert*-butyl)-6-[[bis(2-pyridyl)methyl]amino-methyl]phenol (Htbul), 2,4-di(*tert*-butyl)-6-[[[6-methyl-2-pyridyl)methyl]-(2-pyridyl)methylaminomethyl]phenol (HtbulMepy), and 2,4-di(*tert*-butyl)-6-[[bis(6-methyl-2-pyridyl)methyl]aminomethyl]phenol (Htbul(Mepy)₂), [Zn(tbulCl)] · CH₃OH (**1**), [Zn(tbulMepy)Cl] (**2**), and [Zn(tbul(Mepy)₂)Cl] (**3**), respectively, were prepared and structurally characterized by the X-ray diffraction method. All the complexes were found to have a mononuclear structure with a coordinated phenolate moiety, the geometry of the Zn(II) center being 5-coordinate trigonal-bipyramidal. The Zn(II) binding ability of the ligands with and without 6-methyl-2-pyridylmethyl moieties was evaluated for similar ligands, which lacked the *t*-butyl groups at the 2- and 4-positions of the phenol moiety, by the stability constants determined by potentiometric titration at 25 °C (*I* = 0.1 M (KNO₃)). The stability of the complexes was found to be in the order L > LMepy > L(Mepy)₂, reflecting the steric hindrance of the 6-methyl group of the pyridine ring. Complexes **1**, **2**, and **3** were converted to the phenoxyl radicals upon oxidation with Ce(IV), giving a phenoxyl radical π – π^* transition band at 394–407 nm. ESR and resonance Raman spectra established that the radical species had a Zn(II)–phenoxyl radical bond. The cyclic voltammograms showed similar quasi-reversible redox waves with $E_{1/2}$ = 0.68, 0.67, and 0.63 V (versus Ag/AgCl) for **1**, **2**, and **3**, respectively, corresponding to the formation of the phenoxyl radical, which displayed a first-order decay. The half-lives, 58.6, 25.8, and 15.6 min at –40 °C for **1**, **2**, and **3**, respectively, follow the order of the stability constants of the complexes, indicating that the metal(II)–phenoxyl radical stability is in close relationship with the complexation properties of the present series of N₃O-donor ligands.

© 2008 Elsevier B.V. All rights reserved.

1. Introduction

The protonated and deprotonated forms of the tyrosine phenol moiety play important roles in biological systems and serve as important metal binding sites of metalloenzymes [1–3]. Particularly, redox properties of the metal–phenolate moiety have been intensively studied in recent years due to its occurrence in the active site of galactose oxidase (GOase), which contains one copper ion and performs the oxidation of a primary alcohol to the aldehyde in the presence of dioxygen [1–13]. Many studies have been reported on the nature of the metal–phenoxyl radical bond [12,13]. Since the Zn(II) ion is a redox inactive metal ion [12–16], a number of Zn(II)–phenoxyl radical species have been characterized, and comparative studies using Zn(II)–phenoxyl radical complexes as standards have advanced the understanding of the detail electronic structures of the oxidized metal–phenolate species [12–19].

On the other hand, we reported previously the properties of the phenoxyl radical species obtained by one-electron oxidation of the Cu(II), Ni(II) and Co(III) complexes of some N₃O and N₂O₂ ligands containing pendent phenolate moieties with bulky substituents [19–25]. The oxidation locus on the metal–phenolate complexes was found to be influenced by the donor properties of the ligand nitrogens. For example, oxidation of the ternary Co(III) complexes of N₃O tripodal ligands with a catechol moiety gave different products [20]; upon two-electron oxidation the Co(III) complex having two unsubstituted pyridine rings formed a Co(III)–phenoxyl–semi-quinonate species, whereas the Co(III) complex with two 2-methylpyridine rings gave a Co(III)–phenolate–quinone species. The stability of the Cu(II)–phenoxyl radical from the complexes with N₃O ligands depended upon the donor properties of equatorial nitrogen atoms; with weaker equatorial nitrogen donors, the phenoxyl radical was less stable, and the potential of the phenoxyl radical formation was higher [19]. In contrast, the relationship between the structures of the Ni(II) complexes and decay constants of their phenoxyl radical species was influenced by the number of the 2-methylpyridine moieties, and the radical complex with unsubstituted pyridine rings only exhibited the highest stability,

* Corresponding authors. Tel.: +81 29 228 8374; fax: +81 29 228 8403 (Y. Shimazaki).

E-mail addresses: yshima@mx.ibaraki.ac.jp (Y. Shimazaki), t.yajima@ipcku.kansai-u.ac.jp (T. Yajima).

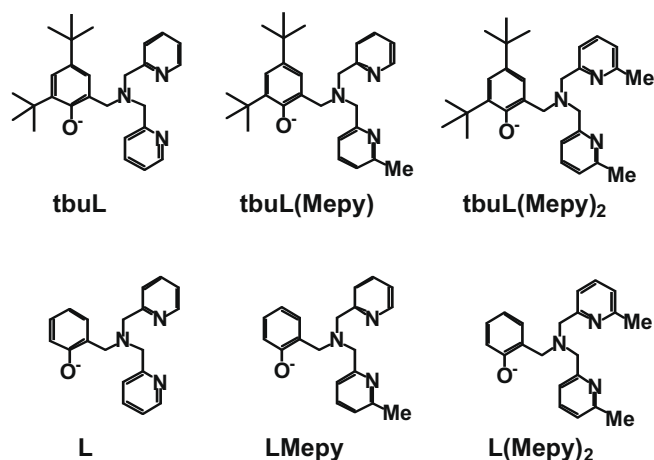


Fig. 1. Structures of ligands in deprotonated form.

which decreased with the increasing number of the 2-methylpyridine moieties [21]. These results suggest that the properties of metal–phenoxyl radical species depend upon the steric hindrance of the pyridine, but the relationship between the nature of the influence of the nitrogen donor properties and the stability and decay processes of the metal–phenoxyl radical species remains to be elucidated.

With these points in mind, we synthesized the Zn(II)–phenolate complexes of a series of N₃O-donor tripodal ligands containing a phenolate moiety with bulky substituents (Fig. 1), chemical and electrochemical generation of the one-electron oxidized phenoxyl radical species in CH₃CN, and characterization of their electronic structures by absorption, ESR, and resonance Raman spectroscopies. We further investigated the influence of the ligand donor ability on the zinc site structure on the basis of the stability constants of the phenolate complexes determined by the potentiometric titration.

2. Experimental

2.1. Materials and methods

All the chemicals used were of the highest grade available and were further purified whenever necessary [26]. Solvents were also purified before use by standard methods [26]. Synthesis of ligands, 2,4-di(*tert*-butyl)-6-[[bis(2-pyridyl)methyl]aminomethyl]phenol (HtbuL; H in this and all other ligands denotes a phenol proton), 2,4-di(*tert*-butyl)-6-[[bis(6-methyl-2-pyridyl)methyl]aminomethyl]phenol (HtbuLMepy), and 2,4-di(*tert*-butyl)-6-[[bis(6-methyl-2-pyridyl)methyl]aminomethyl]phenol (HtbuL(Mepy)₂) (Fig. 1), has been reported previously, and the ligands for potentiometric titration, 2-[[bis(2-pyridyl)methyl]aminomethyl]phenol (HL), 2-[[bis(6-methyl-2-pyridyl)methyl]aminomethyl]phenol (HLMepy), and 2-[[bis(6-methyl-2-pyridyl)methyl]aminomethyl]phenol (HL(Mepy)₂) (Fig. 1), were also synthesized by similar procedures using salicylaldehyde and corresponding secondary amine [19]. Electronic spectra were obtained with a Shimadzu UV-3101PC spectrophotometer. Electrochemical measurements were carried out in a conventional three-electrode cell for samples (1 mM) dissolved in dry CH₃CN containing 0.1 M tetra-*n*-butylammonium perchlorate (TBAP). A glassy-carbon electrode and a platinum wire were used as a working and a counter electrode, respectively, with a Ag/AgCl reference electrode used in all the experiments. The reversibility of the electrochemical processes was obtained by standard procedures and referenced against the

ferrocene/ferricenium redox couple. Frozen solution ESR spectra were acquired by a JEOL JES-RE1X X-band spectrometer equipped with a standard low-temperature apparatus. The spectra were recorded at 77 K by using quartz tubes with a 4-mm inner diameter. Microwave frequency was standardized against a Mn(II) marker. Resonance Raman spectra were measured with a JASCO NR-1800 triple polychromator equipped with a liquid-nitrogen-cooled Princeton Instruments CCD detector. Raman shifts were calibrated with acetone, the accuracy of the peak positions of the Raman bands being ± 1 cm^{−1}.

2.2. Synthesis of complexes

2.2.1. [Zn(tbuL)Cl] · CH₃OH (1)

To a solution of HtbuL (0.417 g, 1.00 mmol) in methanol (10 ml) was added ZnCl₂ (0.136 g, 1.00 mmol), and the resulting solution was mixed with a few drops of triethylamine and left to stand for a few days at room temperature. The colorless microcrystals obtained were recrystallized from CH₃OH. Yield: 0.275 g (65.9%). *Anal. Calc.* for C₂₈H₃₈N₃O₂ClZn: C, 61.21; H, 6.97; N, 7.65. *Found:* C, 61.26; H, 6.99; N, 7.65%. ¹H NMR (CDCl₃, 300 MHz): δ = 1.23(s, 9H), 1.43(s, 9H), 3.78(s, 2H), 3.86(d, 2H), 4.11(d, 2H), 6.79(d, 1H), 7.12(d, 1H), 7.26(d, 2H), 7.43(t, 2H), 7.82(td, 2H), 9.44(d, 2H).

2.2.2. [Zn(tbuLMepy)Cl] (2)

This complex was prepared in a similar manner in 54% yield. *Anal. Calc.* for C₂₈H₃₆N₃OClZn: C, 63.28; H, 6.83; N, 7.91. *Found:* C, 63.33; H, 6.89; N, 8.00%. ¹H NMR (CDCl₃, 300 MHz): δ = 1.14(s, 9H), 1.38(s, 9H), 3.03(d, 1H), 3.16(s, 3H), 3.94(d, 1H), 3.99(d, 1H), 4.08(d, 1H), 4.21(d, 1H), 4.37(d, 1H), 6.65(d, 1H), 6.88(d, 1H), 6.92(d, 1H), 7.12(d, 1H), 7.15(t, 1H), 7.28(d, 1H), 7.54(td, 1H), 7.72(t, 1H), 8.93(d, 1H).

2.2.3. [Zn(tbuL(Mepy)₂)Cl] (3)

This complex was prepared in a similar manner in 56% yield. *Anal. Calc.* for C₂₉H₃₈N₃OClZn: C, 63.86; H, 7.02; N, 7.70. *Found:* C, 63.79; H, 7.05; N, 7.71%. ¹H NMR (CDCl₃, 300 MHz): δ = 1.12(s, 9H), 1.36(s, 9H), 2.87(s, 3H), 3.51(s, 2H), 4.06(d, 1H), 4.36(d, 1H), 6.55(d, 1H), 6.89(d, 1H), 6.91(d, 2H), 7.04(d, 2H), 7.50(t, 2H).

2.3. X-ray structure determination

The X-ray experiments were carried out for the well-shaped single crystals of complexes **1**, **2**, and **3** on a Rigaku RAXIS imaging plate area detector with graphite monochromated Mo K α radiation (λ = 0.71073 Å). The crystals were mounted on a glass fiber. For determination of the cell constants and orientation matrix, three oscillation photographs were taken for each frame with the oscillation angle of 3° and the exposure time of 3 min. Reflection data were corrected for both Lorentz and polarization effects. The structures were solved by the heavy-atom method and refined anisotropically for non-hydrogen atoms by full-matrix least-squares calculations. Each refinement was continued until all shifts were smaller than one third of the standard deviations of the parameters involved. Atomic scattering factors and anomalous dispersion terms were taken from the literature [27]. Hydrogen atoms except for the methanol-OH hydrogen were located at the calculated positions and were assigned a fixed displacement and constrained to ideal geometry with C–H = 0.95 Å. The thermal parameters of calculated hydrogen atoms were related to those of their parent atoms by $U(\text{H}) = 1.2U_{\text{eq}}(\text{C})$. The hydrogen atom of the methanol-OH group of **1** was located from the difference Fourier maps. All the calculations were performed by using the TEXSAN program package [28]. The fundamental crystal data and experimental parameters for structure determination are summarized in Table 1.

Download English Version:

<https://daneshyari.com/en/article/1309881>

Download Persian Version:

<https://daneshyari.com/article/1309881>

[Daneshyari.com](https://daneshyari.com)